



Maxim Yakovlev · Dmitry Kononov

Multiscale geomechanical modeling under finite strains using finite element method

Received: 17 January 2022 / Accepted: 21 April 2022 / Published online: 12 May 2022
© The Author(s), under exclusive licence to Springer-Verlag GmbH Germany, part of Springer Nature 2022

Abstract The article considers an approach for multiscale geomechanical modeling under finite strains. A mathematical model, methods and algorithms for the multiscale numerical estimation of the effective elastic and thermal properties of the preloaded heterogeneous porous materials under finite strains are presented. The developed algorithms were applied to the problem of the estimation of the effective properties of core samples. The digital models obtained from computed tomography scan data of core samples are used. An initial voxel representation of the digital core sample is transformed into an unstructured mesh, thus reducing the number of unknowns by orders of magnitude and requiring computational resources accordingly. The mesh convergence tests demonstrated the efficiency and correctness of the developed algorithms. The calculations of the effective elastic and thermal properties of preloaded porous materials are performed with CAE Fidesys using finite element method. The numerical results demonstrate the significant impact of pre-loading by internal pressure on the effective properties of porous materials.

Keywords Multiscale modeling · Finite strains · Finite element method · Prestress · Core samples

1 Introduction

Multiscale modeling is an effective tool for the analysis of processes in structured media [2,4,8,11,25]. In geomechanics, multiscale analysis is used in [1,3,12,32,33,41]. There are three basic approaches in multiscale modeling [4,8]. The first approach is based on hierarchical methods. These methods use homogenization (upscaling) procedures. The concept of a representative volume element (RVE) is used in this approach, and the stress–strain relations at higher (coarser) scales are derived from the relations at lower (finer) scales taking into account the structure of RVE. The hierarchical methods are divided into one- and two-way coupled methods [38]. The difference between these methods is that in two-way coupled methods, the results of solution at coarser scales are passed to finer scales, and the problems at a fine scale are solved repeatedly for a set of points at a coarse scale. The upscaling methods are widely used in composite mechanics, including finite strain problems [35,36,42]. The difficulties of multiscale modeling in geomechanics are related to the highly nonlinear mechanical properties of geomaterials, structural changes of these materials in time, fluid flow in pores, and other factors [26]. The second approach is a concurrent multiscale analysis. This method uses the decomposition of the total solution into the coarse-scale solution and the fine-scale correction [4,8,38]. The third approach is an introduction of a continuum including complex microstructural effects using higher-gradient models [5,10,30].

Communicated by Andreas Öchsner.

M. Yakovlev (✉) · D. Kononov
Lomonosov Moscow State University, Moscow, Russian Federation
E-mail: maxim.yakovlev@math.msu.ru

In the presented article, the first approach is developed. The issues concerning the application of finite element method to geomechanical modeling at different scales are considered. These issues include:

- a homogenization procedure for finite strains that takes initial pore pressure into account;
- a method for calculating the effective thermophysical properties of inhomogeneous geomaterials;
- a hierarchical approach to the computation of effective characteristics of core samples using the data of computed tomography.

The finite element method is implemented in simulation software CAE Fidesys.

The approach used for homogenization develops the technique is presented in [18,20–23,39,40]. A representative volume which mechanical behavior represents the properties of material as a whole is extracted from the body. The static problem of nonlinear elasticity is solved for this volume at given loads applied to its boundary. Then, the strains and stresses are averaged over the representative volume (area), and the effective constitutive equations are constructed as a relation between the average strains and the average stresses. Effective properties are found in the form of nonlinear constitutive relations for anisotropic materials [17]. The effective constitutive relations are written in an analytical form that is convenient for further use at the next hierarchical level. So, the proposed approach for homogenization at finite strains permits one to obtain the *nonlinear* effective constitutive equations *in explicit analytical form* [18,22,39]. This is an important advantage of the developed method. This approach is used for multiscale analysis of core samples.

The new contribution in the presented article is that the preliminary stresses due to pore pressure are taken into account in the model. The proposed approach is implemented in CAE Fidesys. Periodic cells of arbitrary geometries and relative orientations of holes (fractures) and inclusions can be considered. (Note that analytical models can usually be constructed only for the case of uniformly distributed holes of the same shape and size.) A numerical example is given, and the dependence of effective elastic moduli on pore pressure is analyzed.

A method for the estimation of effective coefficients of thermal expansion and thermal conductivity is proposed. This method based on the finite-element solutions of boundary-value problems of thermoelasticity and thermal conductivity, respectively.

The proposed approach is used in order to estimate effective geomechanical and thermal properties of the rock samples based on their digital models, obtained from the computed tomography (CT) scan data. The computations are performed on a core sample made of oolitic limestone. The internal structure of a core is given in the form of a digital model consisting of cubic cells (voxels). A two-scale estimation of the core sample's effective properties is performed. The need for the two-scale estimation is attributed to the fact that the core sample at the mesolevel contains 4 components, one of which—the unconsolidated rock—is structurally inhomogeneous. A special procedure has been developed for mesh coarsening. This procedure constructs an unstructured tetrahedral mesh based on the given voxel representation of the sample structure. The coarsening of the mesh leads to a reduction in the computational time. In order to maintain high accuracy in computations, a mesh convergence analysis is performed on a fragment of the core sample, and the mesh size for which the accuracy is high enough is determined.

Summing up the introduction, we have to say a few words about what the original contribution of the article is:

- development of an algorithm for numerical estimation of the effective mechanical properties of rocks on the core sample scale using the finite element method;
- when estimating the rock effective properties take physical and geometric nonlinearity and pre-loading into consideration;
- development of an algorithm for numerical estimation of the effective thermal properties (thermal expansion and thermal conductivity coefficients) of rocks on the core sample scale using the finite element method;
- demonstration of the significant impact of pre-loading on the effective elastic properties of porous pressurized materials undergoing finite strains.

2 Numerical estimation of the effective properties of core samples

2.1 Effective elastic properties of core samples

A sample of rock extracted from the depths of the earth by a special kind of drilling is called a core sample. Mechanical and thermal properties of the core samples can be estimated by in situ analysis using different laboratory experiments [7]. However, such experiments take a lot of time and require specialized expensive equipment, and some methods involve destruction of core samples during experiments.

An alternative is the method of computed tomography (CT) which allows obtaining information about the internal structure of a core in the form of a digital model consisting of cubic cells (voxels). Interpretation of CT images results in a decomposition of voxels in the following subdomains: a mineral, kerogen, fluid, or void (pores) space. Such voxel models are further used to estimate the effective mechanical and thermal properties of a core sample by numerical solving of the elasticity and thermal conductivity problems using the finite element method (FEM).

The effective properties of a core sample are estimated in a nonlinear form (under finite strains), taking possible preloading of a core sample into account, and also reducing the dimension (in some cases by 2-3 orders of magnitude) of the problem (the number of nodes in the mesh) by constructing a digital core model (reconstructed geometry) and an unstructured mesh for its discretization based on the original voxel model obtained from the CT scan results.

The approach to deriving effective properties of core samples has the following basic principles. **The representative volume element (RVE)** of core sample is the minimal volume of the core, that can be used for the experiments and measurements, on the basis of which it is possible to make conclusions about the behavior of the core as a whole. The RVE should contain a sufficient volume of each mineral [37] in order to have a possibility of averaging the properties of the entire core.

We begin with the definition of the effective elastic properties of a core sample. Let's call the homogeneous material **as the effective (averaged) material** (from the point of view of *elasticity*), if it meets the following condition: if we consider a RVE of the initial core in the form of a rectangular parallelepiped in the undeformed configuration and fill the same volume with this homogeneous material, then the averaged stresses over the volume in the initial core and the homogeneous effective material will be equal for the equal displacements of bounds.

Let's describe an algorithm for the estimation of the effective elastic properties of the core sample using this definition [13, 18, 20, 21, 39]. We solve a set of the elasticity theory boundary-value problem sets [19, 24, 27] for a RVE V_0 in the form of a rectangular parallelepiped that was selected in the initial state (before deformation):

$$\nabla \cdot \boldsymbol{\sigma} = 0 \text{ or } \overset{0}{\nabla} \cdot \mathbf{P} = 0 \quad (1)$$

with boundary conditions (BCs)

$$\mathbf{u} \Big|_{\Gamma_0} = (\mathbf{F}^e - \mathbf{I}) \cdot \overset{0}{\mathbf{R}} \quad (2)$$

Here \mathbf{I} is the identity tensor, $\overset{0}{\nabla}$, ∇ are the gradient operators in the initial and current states (configurations), $\overset{0}{\mathbf{R}}$, \mathbf{R} are the radius-vectors of a particle in the initial and current states, respectively; $\mathbf{u} = \mathbf{R} - \overset{0}{\mathbf{R}}$ is the displacement vector, Γ_0 is the bound of the RVE in the initial state, $\mathbf{F} = \left(\overset{0}{\nabla} \mathbf{R} \right) = \left(\mathbf{I} + \overset{0}{\nabla} \mathbf{u} \right) = (\nabla \mathbf{r})^{-1} = (\mathbf{I} - \nabla \mathbf{u})^{-1}$ is the deformation gradient, $\boldsymbol{\sigma}$ is the true stress tensor, $\mathbf{P} = (\det \mathbf{F}) \boldsymbol{\sigma} \cdot (\mathbf{F}^T)^{-1}$ is the first Piola-Kirchhoff stress tensor, and \mathbf{F}^e is the deformation gradient of the effective material. The superscript T denotes transposition.

Each problem set matches a certain type of strain and a certain form of the Green strain tensor [18, 39]. Solving each problem of each set using FEM or SEM, we get a field of the true stress tensor $\boldsymbol{\sigma}$. Knowing this tensor, we calculate the effective stress tensor $\boldsymbol{\sigma}^e$ using an averaging of $\boldsymbol{\sigma}$ over the volume V in the current configuration:

$$\boldsymbol{\sigma}^e = \frac{1}{V} \int_V \boldsymbol{\sigma} dV \quad (3)$$

Knowing the deformation gradient \mathbf{F}^e (which we set), we can now calculate the effective Green strain tensor:

$$\overset{0}{\mathbf{E}}^e = \frac{1}{2} (\mathbf{F}^{eT} \cdot \mathbf{F}^e - \mathbf{I}) \quad (4)$$

In the linear case, we derive the effective constitutive equations as linear relations between the true stress tensor $\boldsymbol{\sigma}^e$ and the Green strain tensor:

$$\sigma_{ij}^e = C_{ijkl} E_{kl}^e \quad (5)$$

In the nonlinear case, knowing σ^e , we first calculate the effective second Piola–Kirchhoff stress tensor \mathbf{S}^e by the formula:

$$\mathbf{S}^e = (\det \mathbf{F}^e) (\mathbf{F}^e)^{-1} \cdot \sigma^e \cdot (\mathbf{F}^e)^{T-1} \quad (6)$$

and we derive the effective properties in the form of a quadratic relation between the second Piola–Kirchhoff stress tensor \mathbf{S}^e and the Green tensor \mathbf{E}^e :

$$S_{ij}^e = C_{ijkl}^{(0)} E_{kl}^e + C_{ijklmn}^{(1)} E_{kl}^e E_{mn}^e \quad (7)$$

Thus, the problem of the estimation of effective linear-elastic properties of the core sample is reduced to computing the coefficients C_{ijkl} , and the problem of the estimation of effective nonlinear-elastic properties is reduced to the calculation of the coefficients $C_{ijkl}^{(0)}$ and $C_{ijklmn}^{(1)}$ [23].

The main point of the above-described algorithm for estimating the effective elastic properties of the core samples is as follows: an unstressed RVE (i.e., a RVE which average strains and stresses are initially equal to zero) undergoes certain mechanical actions that cause some average strains, which result in some average stresses in the model. The relationship between the resulting average stresses and strains makes it possible to estimate the effective elastic properties of the core.

Sometimes it is necessary to numerically estimate the effective properties of the core subjected to prestress, for example, stressed by pore pressure. If the problem is solved in the linear case, such prestress will not affect the effective elastic properties of the core in accordance with the principle of superposition. Therefore, we describe the approach to the estimation of the effective elastic properties of the prestressed core sample under finite strains, taking into account geometrical and physical nonlinearities.

There're several differences with respect to the technique described in the previous paragraph. For a RVE, a number of boundary-value problems of the nonlinear elasticity are similarly solved. However, in addition to boundary conditions in each problem, there're also boundary conditions or stresses corresponding to the prestress of the RVE. Furthermore, a separate problem is solved for RVE. In this additional problem, stresses corresponding to the prestress of the material are provided, however the effective deformation gradient \mathbf{F}^e is the identity tensor. So, the effective Green stress tensor \mathbf{E}^e is equal to zero—thus, the average strains in the model are equal to zero. However, prestressing results in nonzero average stresses. The true stress tensor σ_0^e for the additional problem is calculated by integrating over the volume. Using known σ_0^e , the average second Piola–Kirchhoff stress tensor \mathbf{S}_0^e is calculated.

After solving all boundary-value problems and the additional problem with zero average strain and prestress for the RVE and averaging the stresses, the effective nonlinear-elastic properties of the core are estimated as a quadratic dependence of the difference between \mathbf{S}^e and \mathbf{S}_0^e on the Green stress tensor \mathbf{E}^e :

$$S_{ij}^e - S_{0,ij}^e = C_{ijkl}^{(0)} E_{kl}^e + C_{ijklmn}^{(1)} E_{kl}^e E_{mn}^e \quad (8)$$

The essence of the described approach is that the prestress creates some strains and stresses (natural ones) in a RVE, and, after prestressing, additional (artificial) average strains are applied to the model, causing additional (artificial) average stresses. The effective properties of the prestressed material represent the relationship between these additional stresses and strains.

After the computation of effective moduli using the proposed approach, the averaging of these moduli over all directions can be performed [18]. This procedure permits one to obtain the effective constitutive equations for isotropic materials. As a result, the relation (7) is reduced to the Murnaghan constitutive equation [27]. For linear elastic materials (see Eq. 5), Young's modulus and Poisson's ratio are determined.

This method of numerical estimation of the effective nonlinear-elastic properties of prestressed heterogeneous materials is implemented in the software module *Fidesys Composite* of CAE Fidesys. Boundary-value problems of nonlinear elasticity are solved by FEM [23, 39] or SEM [13]. As an example, we present further numerical results for the problem of estimating the effective nonlinear-elastic properties of the porous material

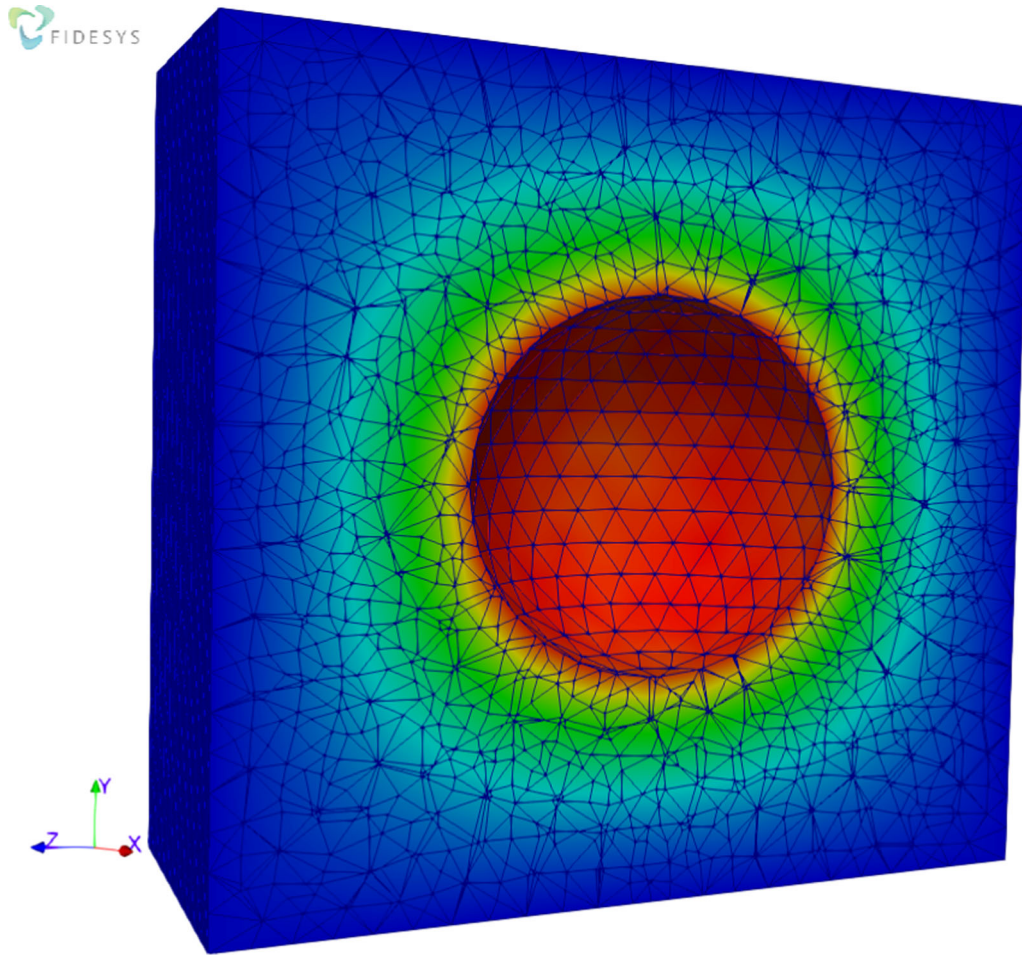


Fig. 1 The representative volume with a pore

[6] prestressed by pore pressure (Fig. 1). The mechanical properties of the solid material are described by constitutive equation for the Murnaghan potential

$$\overset{0}{\mathbf{S}} = \lambda (\overset{0}{\mathbf{E}} : \mathbf{I}) + 2G \overset{0}{\mathbf{E}} + 3C_3 (\overset{0}{\mathbf{E}} : \mathbf{I})^2 \mathbf{I} + C_4 (\overset{0}{\mathbf{E}}^2 : \mathbf{I}) \mathbf{I} + 2C_4 (\overset{0}{\mathbf{E}} : \mathbf{I}) \overset{0}{\mathbf{E}} + 3C_5 \overset{0}{\mathbf{E}}^2 \quad (9)$$

with the constants $\lambda = 1.09 \cdot 10^5$ MPa, $G = 0.818 \cdot 10^5$ MPa, $C_3 = -0.29 \cdot 10^5$ MPa, $C_4 = -2.4 \cdot 10^5$ MPa, $C_5 = -2.25 \cdot 10^5$ MPa.

Calculations show that by varying the pore pressure from zero to 14 GPa the coefficient $C_{1122}^{(0)}$ decreases by 10% (from 66 to 60 GPa), and the coefficient $C_{111122}^{(1)}$ increases by 15% in absolute value (Fig. 2).

It indicates the need to take into account the prestress for the numerical estimation of effective properties.

2.2 Effective thermal properties of core samples

Let's define the effective thermal expansion of core sample. Let's call the homogeneous material **as the effective (averaged) material** (from the point of view of *thermal expansion*), if it meets the following condition: if we consider a RVE of the initial core in the form of a rectangular parallelepiped allocated in the undeformed configuration and fill the same volume with the homogeneous material, then the averaged thermal strains over the volume in source core and the homogeneous effective material will be equal for the equal temperature distribution over the volumes.

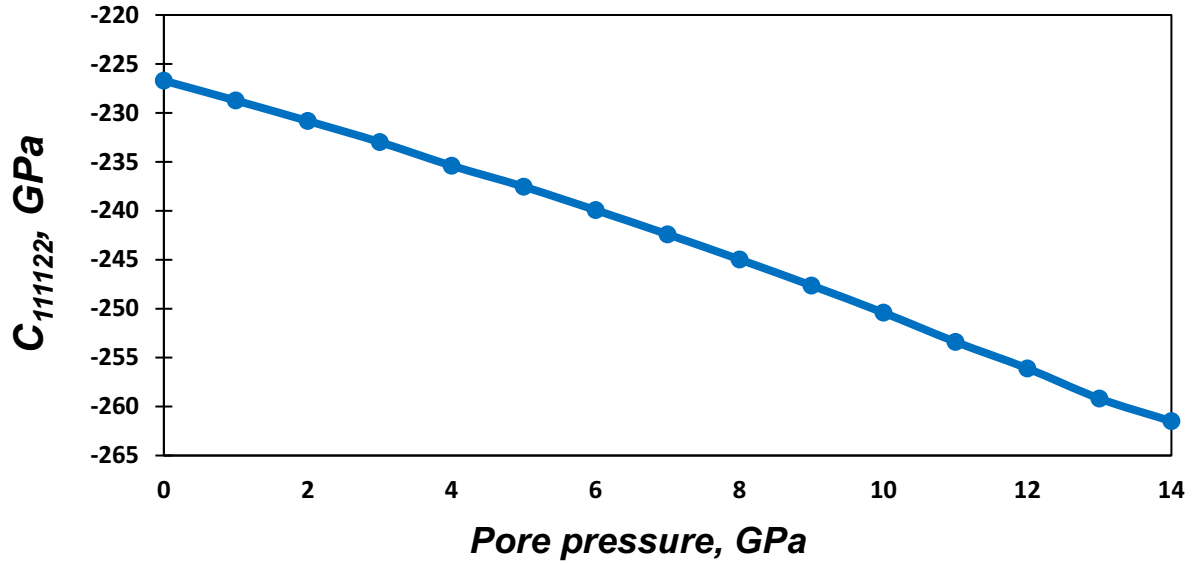


Fig. 2 The dependence of coefficient $C_{111122}^{(1)}$ on pore pressure

Let's describe an algorithm for estimation of the effective thermal expansion of the core sample using this definition [40]. We consider the thermal expansion for a RVE V_0 in the form of a rectangular parallelepiped that was chosen in its initial (undeformed) state to solve a boundary-value problem of thermoelasticity:

$$\begin{aligned} \nabla \cdot \boldsymbol{\sigma}^{el} &= 0 \\ \boldsymbol{\sigma}^{el} &= \boldsymbol{\sigma} - \boldsymbol{\sigma}^{th} \end{aligned} \quad (10)$$

where $\boldsymbol{\sigma}$ is a total (true) stress tensor, $\boldsymbol{\sigma}^{el}$ is the mechanic (elastic) stress tensor, $\boldsymbol{\sigma}^{th}$ is the thermal stress tensor.

Boundary conditions are zero pressure, which allows the RVE to expand freely as the temperature increases. The entire volume is heated at ΔT and expanded. By averaging the total strain tensor over the volume (in the deformed state), we obtain the effective strain tensor:

$$\boldsymbol{\varepsilon}^e = \frac{1}{V} \int_V \boldsymbol{\varepsilon} dV \quad (11)$$

We derive the effective thermal expansion tensor of the core sample using linear relations between the effective strain tensor $\boldsymbol{\varepsilon}^e$ and ΔT :

$$\varepsilon_{ij}^e = \alpha_{ij} \Delta T \quad (12)$$

Effective thermal expansion coefficients can be found from the formula:

$$\alpha_{ij} = \frac{\varepsilon_{ij}^e}{\Delta T} \quad (13)$$

Finally, let's define the effective thermal conductivity [9] of a core sample. Let's call the homogeneous material **as the effective (averaged) material** (from the point of view of *thermal conductivity*), if it meets the following condition: if we consider a RVE of the initial core in the form of a rectangular parallelepiped and fill the same volume with the homogeneous material, then the averaged heat flow over the volume in the initial core sample and the homogeneous effective material will be equal for the equal temperature gradients specified at the boundary.

Let's describe an algorithm for the estimation of the effective thermal conductivity of the core sample using this definition [40]. We solve a number of boundary-value thermal problems for a RVE V_0 in the form of a rectangular parallelepiped (for steady thermal state with no internal heat sources):

$$\nabla \cdot \mathbf{q} = 0 \quad (14)$$

with the predefined temperature at the boundary:

$$T|_{\Gamma} = \nabla T^e \cdot \mathbf{r} \quad (15)$$

where \mathbf{q} is a heat flux vector and ∇T^e is the effective temperature gradient on the RVE. Each boundary-value problem of thermal conductivity matches to a certain form of the effective temperature gradient.

Solving each problem using FEM or SEM, we obtain a field of the heat flux vector \mathbf{q} . Furthermore, we calculate the effective heat flux vector \mathbf{q}^e by averaging of \mathbf{q} over volume:

$$\mathbf{q}^e = \frac{1}{V} \int_V \mathbf{q} dV \quad (16)$$

We derive the effective thermal conductivity of the core sample as linear relations between the effective heat flux vector \mathbf{q}^e and the effective temperature gradient ∇T^e (accordingly to Fourier law of thermal conductivity):

$$q_i^e = -\lambda_{ij} (\nabla T^e)_j \quad (17)$$

So, the problem of the estimation of effective thermal conductivity of the core sample is reduced to computing the coefficients λ_{ij} .

2.3 Results

We investigate the effective elastic properties of two core samples of oolitic limestone. CT scan data in the form of voxel models (voxel size is **264.58 μm** , mesoscale) is provided by Geological department of Lomonosov Moscow State University. Both core samples have a cuboidal shape. The voxel model of the first sample has dimensions of $320 \times 320 \times 1171$ voxels, and the voxel model of the second sample has dimensions of $320 \times 320 \times 976$ voxels. So, the voxel mesh for each sample contains approximately 100 million elements. Both core samples contain 4 components: pyrite, calcite, unconsolidated rock and pores (voids). The mechanical properties of pyrite and calcite are provided, while the unconsolidated rock is actually a porous calcite. Its micro CT scan data was also provided (the voxel size is **0.8 μm** , microscale). We numerically estimated the effective properties of the unconsolidated rock to use these properties when estimating the effective properties of full-sized core samples at mesoscale. Thus, the two-scale estimation of core sample effective properties was done (Fig. 3). A fragment of a full-size core at the mesoscale (the voxel size is 264.58 μm) is shown on the left-hand side of this figure. The size of this fragment is $100 \times 100 \times 100$ voxels. The red color in this image corresponds to pyrite, the gray color—to solid calcite, and the blue color—to porous calcite. A fragment of the unconsolidated rock at the microscale (the voxel size is 0.8 μm) is shown on the left-hand side of Fig. 3. The size of this fragment is $200 \times 200 \times 200$ voxels.

For calcite, we used the Young's modulus of 80.4 GPa and Poisson's ratio of 0.32. We estimated the properties of the unconsolidated rock on a Cartesian hexahedral mesh coinciding with the voxel model obtained by CT scanning (8 million elements). The computations are performed using the method described in Sect. 2.1 for the case of linear elasticity. The effective material turns out to be roughly isotropic with Young's modulus of 31.75 GPa and Poisson's ratio of 0.29 (the fragment's porosity is 30.8%).

After estimating the unconsolidated rock properties, we calculated the effective properties of the full-size core samples. For pyrite, we used Young's modulus of 291.2 GPa and Poisson's ratio of 0.16. The problem appears to be due to a very large number of elements in the initial voxel mesh. In order to overcome this difficulty without using a supercomputer, an unstructured tetrahedral mesh (Fig. 4) is constructed. The construction of this mesh is performed for both core samples by the mesh generation tools of CAE Fidesys using the initial voxel models. This approach allows to obtain an unstructured mesh consisting of several million tetrahedra. However, the following question naturally occurs: how do the effective properties calculated on the unstructured mesh correspond to the effective properties computed on the original model? In order to verify this, the mesh convergence analysis was done on fragments of core samples.

The verification is carried out by a series of calculations on the fragments of $100 \times 100 \times 100$ voxels for both oolitic limestone core samples (for the first core sample this fragment is shown in Fig. 3 on the left). The results of verification are given in Table 1. The table shows the relative error of the Young modulus for different meshes.

The table shows that the results on a tetrahedral mesh are in good agreement with the results on the voxel model already on the mesh of about 5000 tetrahedra. These results prove the applicability and sufficiently high

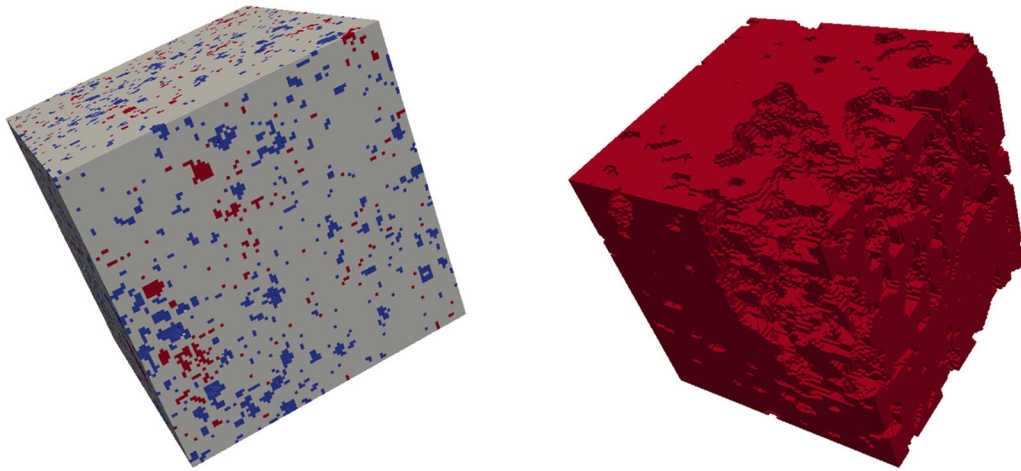


Fig. 3 (Left) A fragment of a full-size core containing three rocks (voxel size is 264.58 μm , mesoscale). (Right) A fragment of the unconsolidated rock (voxel size is 0,8 μm , microscale)

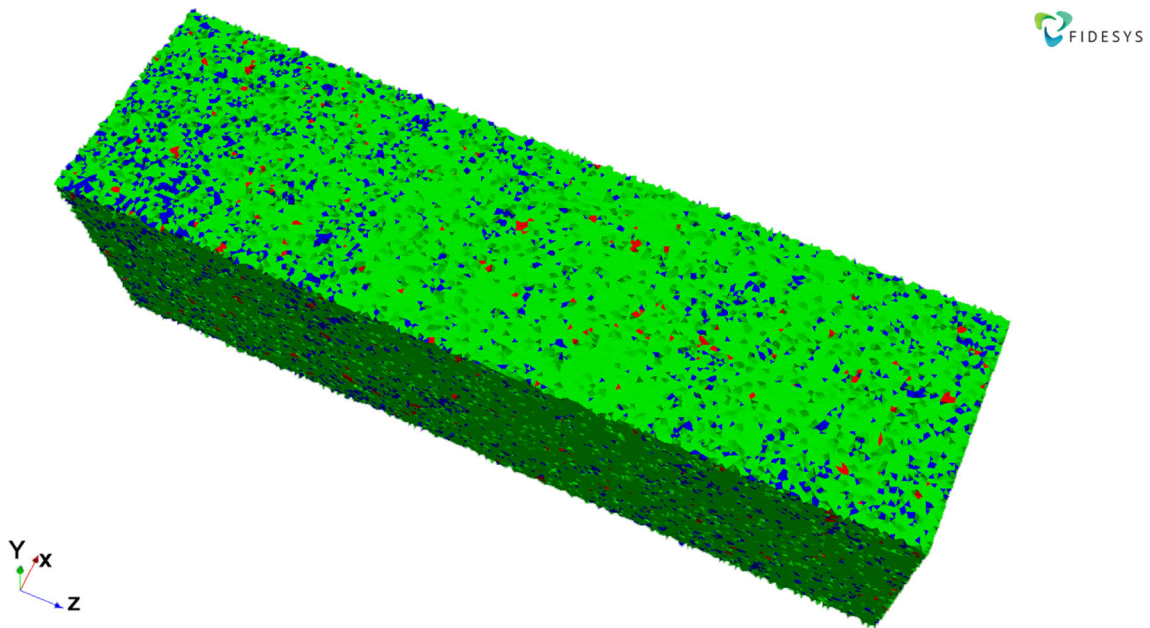


Fig. 4 An unstructured tetrahedral mesh built for a full-size core sample containing three types of rocks, based on the initial voxel model. The red color corresponds to pyrite, the green color—to solid calcite, and the blue color—to porous calcite (color figure online)

efficiency of the suggested approach for full-size core samples. (A Cartesian hexahedral mesh based on the voxel model containing about 100 million nodes is replaced by an unstructured tetrahedral mesh containing thousands of nodes.)

For full-sized core samples, the effective properties are computed on successively refined tetrahedral meshes in order to investigate the mesh convergence. The results for the first full-sized core sample ($320 \times 320 \times 1171$ voxels) are presented in Table 2.

One can see from Table 2 that a good mesh convergence is achieved for the effective moduli. The converged effective properties are the following: the effective Young's modulus is **78.13 GPa**, Poisson's ratio is **0.32**.

These obtained results are of physical sense as they're close to the properties of calcite in the solid (consolidated) phase, which is the main component of both core samples.

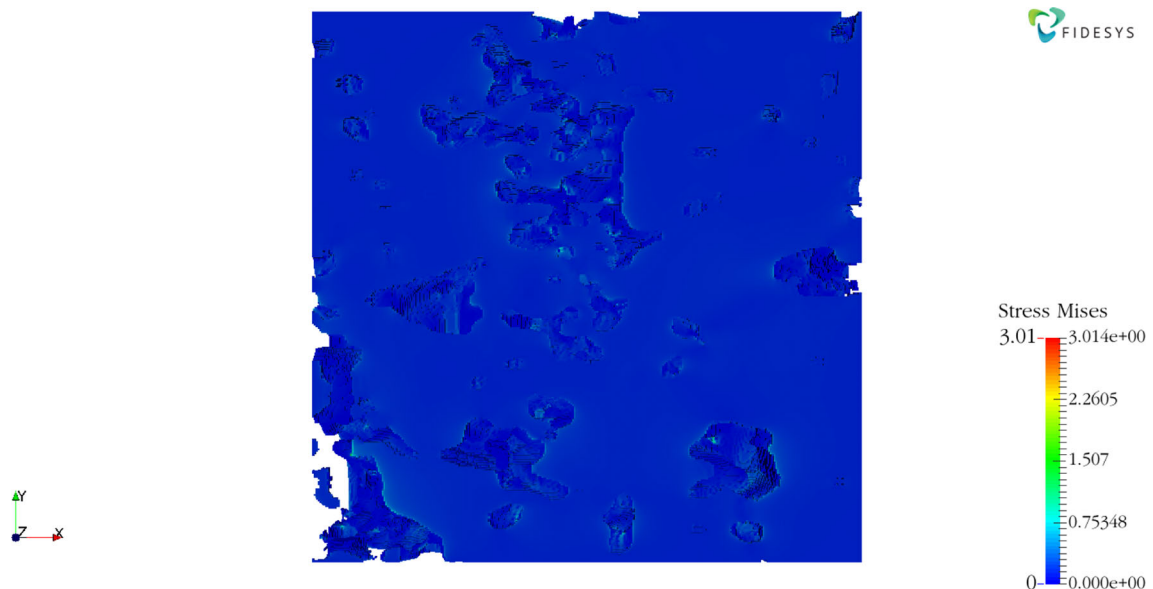
The effective thermal properties of another core sample containing a single rock (sandstone) and pores are investigated. The porosity of the core sample is 20.8%. Sandstone has Young's modulus of 70 GPa,

Table 1 The results of computation of effective elastic properties on a series of meshes for the fragment $100 \times 100 \times 100$ voxels of a core sample

Coarsening factor	Number of nodes	Number of elements	Relative error, %
0.01	895,654	5,286,753	0.31
0.02	131,220	752,411	0.41
0.03	40,680	227,476	1.01
0.04	16,698	91,137	1.61
0.05	9307	49,700	1.16
0.06	5798	29,253	0.49
0.07	3376	16,782	0.49
0.08	2352	11,521	1.29
0.09	1717	8337	1.30
0.1	1151	5413	0.77
Voxel model	1,020,100	984,274	

Table 2 The results of computation of effective elastic properties on a series of meshes for the full-sized core sample

Coarsening factor	Number of nodes	Number of elements	Young's modulus, GPa	Poisson's ratio
0.015	1,188,440	7,038,265	78.134	0.316
0.02	486,845	2,862,912	78.399	0.316
0.03	148,939	859,912	78.238	0.315
0.04	64,738	366,361	77.797	0.315
0.05	33,860	187,752	77.215	0.315

**Fig. 5** The stress distribution in the investigated fragment of the core sample made of porous sandstone

Poisson's ratio of 0.15, linear thermal expansion coefficient of 10^{-5} K^{-1} , and thermal conductivity coefficient of 1.5 W/m K. The calculations are done for a sandstone fragment of $300 \times 300 \times 300$ voxels, directly on the voxel model (without rebuilding a tetrahedral mesh). The stress distribution in the fragment is shown in Fig. 5.

The following effective properties are obtained: the linear thermal expansion coefficient is $0.997 \cdot 10^{-5} \text{ K}^{-1}$ and the thermal conductivity coefficient is 1.052 W/m K .

3 Conclusion

In the article, an approach for the numerical estimation of the effective elastic and thermal properties of the preloaded heterogeneous porous materials under finite strains is presented. The developed method of homoge-

nization permits one to write effective constitutive equations for porous nonlinear-elastic materials under finite strains with account of prestress due to pore pressure. Boundary-value problems are solved using the finite element method implemented in CAE Fidesys. The numerical results presented in the article demonstrate the significant impact of pre-loading on the effective elastic properties of porous pressurized materials undergoing finite strains. The developed algorithms were applied to the multiscale problem of the estimation of effective properties of core samples by performing simulations on their digital models obtained from CT scan data. An approach to transformation of initial voxel representation of the digital core sample into unstructured mesh has been developed and verified. This approach permits one to reduce the number of unknowns and required computational resources by orders of magnitude. The mesh convergence tests demonstrated efficiency and correctness of the developed algorithms.

The proposed approaches can be further developed within the framework of two-way hierarchical modeling of geomechanical processes. When the problem is solved at the macrolevel, the determined strains or stresses in a set of points can be transmitted to the finer level, where the stresses and displacements in the core samples disposed in these points can be computed. So, one can observe how the shapes of micropores and microcracks in these core samples change due to loading. By solving the hydrodynamical problems at the finer (micro- or meso-) level and accounting for these changes, one can calculate how the permeability of rock changes due to loading at the given points at the macrolevel [28].

In addition, the developed methods can be used for multiscale modeling of geomechanical processes under superimposed finite strains [22]. One can assume that the structure of the solid material is changed in the process of loading. For example, pores and (or) inclusions may be present in the material (i.e., the mechanical properties of the material may be changed in some regions). Another application is related to the modeling of residual stresses in metamorphic rocks [14–16]. Further investigations could be focused on the computation of effective properties within the framework of the couple stress theory [34] and the homogenization of fluid–structure interaction [5,29,31].

Acknowledgements The research for this article was performed at Lomonosov Moscow State University and was financially supported by the Ministry of Education and Science of the Russian Federation under the agreement $\mathcal{N}_{\circ}075-15-2019-1890$ (with respect to analysis of the effective mechanical properties of core samples, including the case of pre-loading) and as part of the program of the Mathematical Center for Fundamental and Applied Mathematics under the agreement $\mathcal{N}_{\circ}075-15-2019-1621$ (with respect to 3D voxel model creation) and also by the Russian Science Foundation under grant 19-71-10008 (with respect to analysis of the effective thermal properties).

The authors are grateful to Professor of Lomonosov Moscow State University Vladimir Levin for the problem statement and for constant attention to this work.

References

1. Burov, E., Watts, T., Podladchikov, Y., Evans, B.: Observational and modeling perspectives on the mechanical properties of the lithosphere. *Tectonophysics* **631**, 1–3 (2014). <https://doi.org/10.1016/j.tecto.2014.06.010>
2. Da Silva, H.G., Vasylevskiy, K., Drach, B., Tsukrov, I.: Applicability of two-step homogenization to high-crimp woven composites. *Compos. Struct.* **226**, 111157 (2019). <https://doi.org/10.1016/j.compstruct.2019.111157>
3. Daly, K.R., Keyes, S.D., Roose, T.: Determination of macro-scale soil properties from pore scale structures: image-based modelling of poroelastic structures. *Proc. R. Soc. A* **474**, 20170745 (2018). <https://doi.org/10.1098/rspa.2017.0745>
4. De Borst, R.: Challenges in computational materials science: multiple scales, multi-physics and evolving discontinuities. *Comput. Mater. Sci.* **43**, 1–15 (2008). <https://doi.org/10.1016/j.commatsci.2007.07.022>
5. Dell’Isola, F., Guarascio, M., Hutter, K.: A variational approach for the deformation of a saturated porous solid. A second-gradient theory extending Terzaghi’s effective stress principle. *Arch. Appl. Mech.* **70**, 323–337 (2000). <https://doi.org/10.1007/s004199900020>
6. Dell’Isola, F., Madeo, A., Seppecher, P.: Boundary conditions at fluid-permeable interfaces in porous media: a variational approach. *Int. J. Solids Struct.* **46**(17), 3150–3164 (2009). <https://doi.org/10.1016/j.ijsolstr.2009.04.008>
7. Dubinya, N., Tikhotsky, S., Bayuk, I., Beloborodov, D., Krasnova, M., Makarova, A., Rusina, O., Fokin, I.: Prediction of physical-mechanical properties and in-situ stress state of hydrocarbon reservoirs from experimental data and theoretical modelling. In: *SPE Russian Petroleum Technology Conference*. SPE-187823-MS (2017). <https://doi.org/10.2118/187823-MS>
8. Fish, J., Shek, K.: Multiscale analysis of composite materials and structures. *Compos. Sci. Technol.* **60**, 2547–2556 (2000)
9. Giorgio, I.: A variational formulation for one-dimensional linear thermo-viscoelasticity. *Math. Mech. Complex Syst.* **9**(4), 397–412 (2021). <https://doi.org/10.2140/memocs.2021.9.397>
10. Giorgio, I., Andraus, U., dell’Isola, F., Lekszycki, T.: Viscous second gradient porous materials for bones reconstructed with bio-resorbable grafts. *Extreme Mech. Lett.* **13**, 141–147 (2017). <https://doi.org/10.1016/j.eml.2017.02.008>
11. Javanbakht, M., Ghaedi, M.S., Barchiesi, E., Ciallella, A.: The effect of a pre-existing nanovoid on martensite formation and interface propagation: a phase field study. *Math. Mech. Solids* **26**(1), 90–109 (2021). <https://doi.org/10.1177/1081286520948118>

12. Jouini, M.S., Vega, S., Al-Ratrou, A.: Numerical estimation of carbonate rock properties using multiscale images. *Geophys. Prospect.* **63**, 405–421 (2015). <https://doi.org/10.1111/1365-2478.12156>
13. Konovalov, D., Yakovlev, M.: Numerical estimation of effective elastic properties of elastomer composites under finite strains using spectral element method with CAE Fidesys. *Chebyshevskii sbornik* **17**(3), 316–329 (2017). <https://doi.org/10.22405/2226-8383-2017-18-3-316-329> <https://doi.org/10.22405/2226-8383-2017-18-3-316-329>
14. Mazzucchelli, M.L., Angel, R.J., Alvaro, M.: EntraPT: an online platform for elastic geothermobarometry. *Am. Miner.* **106**(5), 830–837 (2021). <https://doi.org/10.2138/am-2021-7693CCBYNCND>
15. Moulas, E., Kostopoulos, D., Podladchikov, Y., et al.: Calculating pressure with elastic geobarometry: a comparison of different elastic solutions with application to a calc-silicate gneiss from the Rhodope Metamorphic Province. *Lithos* **2020**, 105803 (2020). <https://doi.org/10.1016/j.lithos.2020.105803>
16. Murri, M., Mazzucchelli, M.L., Campomenosi, N., Korsakov, A.V., Prencipe, M., Mihailova, B.D., Scambelluri, M., Angel, J.R., Alvlvaro, M.: Raman elastic geobarometry for anisotropic mineral inclusions. *Am. Miner.* **103**, 1869–1872 (2018). <https://doi.org/10.2138/am-2018-6625CCBY>
17. La Valle, G., Massoumi, S.: A new deformation measure for micropolar plates subjected to in-plane loads. *Contin. Mech. Thermodyn.* **34**(1), 243–257 (2022). <https://doi.org/10.1007/s00161-021-01055-7>
18. Levin, V., Lokhin, V., Zingerman, K.: Effective elastic properties of porous materials with randomly dispersed pores. Finite deformation. *Trans. ASME J. Appl. Mech.* **67**(4), 667–670 (2000). <https://doi.org/10.1115/1.1286287>
19. Levin, V.A., Podladchikov, Y.Y., Zingerman, K.M.: An exact solution to the Lamé problem for a hollow sphere for new types of nonlinear elastic materials in the case of large deformations. *Eur. J. Mech. A. Solids* **90**, 104345 (2021). <https://doi.org/10.1016/j.euromechsol.2021.104345>
20. Levin, V., Vdovichenko, I., Vershinin, A., Yakovlev, M., Zingerman, K.: Numerical estimation of effective mechanical properties for reinforced Plexiglas in the two-dimensional case. *Model. Simul. Eng.* **2016**, 9010576 (2016)
21. Levin, V., Vdovichenko, I., Vershinin, A., Yakovlev, M., Zingerman, K.: An approach to the computation of effective strength characteristics of porous materials. *Lett. Mater.* **7**(4), 806–816 (2017). <https://doi.org/10.22226/2410-3535-2017-4-452-454> <https://doi.org/10.22226/2410-3535-2017-4-452-454>
22. Levin, V., Zingermann, K.: Effective constitutive equations for porous elastic materials at finite strains and superimposed finite strains. *Trans. ASME J. Appl. Mech.* **70**(6), 809–816 (2003). <https://doi.org/10.1115/1.1630811>
23. Levin, V., Zingerman, K., Vershinin, A., Yakovlev, M.: Numerical analysis of effective mechanical properties of rubber-cord composites under finite strains. *Compos. Struct.* **131**, 25–36 (2015). <https://doi.org/10.1016/j.compstruct.2015.04.037>
24. Levin, V.A., Zubov, L.M., Zingerman, K.M.: An exact solution to the problem of biaxial loading of a micropolar elastic plate made by joining two prestrained arc-shaped layers under large strains. *Eur. J. Mech. A. Solids* **88**, 104237 (2021). <https://doi.org/10.1016/j.euromechsol.2021.104237>
25. Levitas, V.I.: High-pressure mechanochemistry: conceptual multiscale theory and interpretation of experiments. *Phys. Rev. B* **70**, 184118 (2004). <https://doi.org/10.1103/PhysRevB.70.184118>
26. Liang, W., Zhao, J.: Multiscale modeling of large deformation in geomechanics. *Int. J. Numer. Anal. Methods Geomech.* **43**, 1080–1114 (2019). <https://doi.org/10.1002/nag.2921>
27. Lurie, A.: *Nonlinear Theory of Elasticity*. North-Holland, Amsterdam (1990)
28. Miftakhov, R.F., Myasnikov, A.V., Vershinin, A.V., Chugunov, S.S., Zingerman, K.M.: On a hydro-geomechanical modeling of shale formations. *Seismic Technol.* **4**, 97–108 (2015). <https://doi.org/10.18303/1813-4254-2015-4-97-108>
29. Rohan, E., Lukeš, V.: Modeling large-deforming fluid-saturated porous media using an Eulerian incremental formulation. *Adv. Eng. Softw.* **113**, 84–95 (2017). <https://doi.org/10.1016/j.advengsoft.2016.11.003>
30. Scerrato, D., Bersani, A.M., Giorgio, I.: Bio-inspired design of a porous resorbable scaffold for bone reconstruction: a preliminary study. *Biomimetics* **6**(1), 18 (2021). <https://doi.org/10.3390/biomimetics6010018>
31. Sciarra, G., dell’Isola, F., Hutter, K.: A solid-fluid mixture model allowing for solid dilatation under external pressure. *Contin. Mech. Thermodyn.* **13**, 287–306 (2001). <https://doi.org/10.1007/s001610100053>
32. Semnani, S.J., White, J.A.: An inelastic homogenization framework for layered materials with planes of weakness. *Comput. Methods Appl. Mech. Eng.* **370**, 113221 (2020). <https://doi.org/10.1016/j.cma.2020.113221>
33. Shen, W., Shao, J.: Multiscale modeling approaches and micromechanics of porous rocks. In: Shojaei, A.K., Shao, J. (eds.) *Porous Rock Fracture Mechanics with Application to Hydraulic Fracturing, Drilling and Structural Engineering*, pp. 215–232. Woodhead Publishing, Sawston (2017). <https://doi.org/10.1016/B978-0-08-100781-5.00010-5>
34. Skrzat, A., Eremeyev, V.A.: On the effective properties of foams in the framework of the couple stress theory. *Contin. Mech. Thermodyn.* **32**, 1779–1801 (2020). <https://doi.org/10.1007/s00161-020-00880-6>
35. Song, D., Ponte, Castañeda P.: A multi-scale homogenization model for fine-grained porous viscoplastic polycrystals: I—finite-strain theory. *J. Mech. Phys. Solids* **115**, 102–122 (2018). <https://doi.org/10.1016/j.jmps.2018.03.001>
36. Song, D., Ponte, Castañeda P.: A multi-scale homogenization model for fine-grained porous viscoplastic polycrystals: II—applications to FCC and HCP materials. *J. Mech. Phys. Solids* **115**, 77–101 (2018). <https://doi.org/10.1016/j.jmps.2018.03.002>
37. Spagnuolo, M., Yildizdag, M.E., Pinelli, X., Cazzani, A., Hild, F.: Out-of-plane deformation reduction via inelastic hinges in fibrous metamaterials and simplified damage approach. *Math. Mech. Solids* (2002). <https://doi.org/10.1177/10812865211052670>
38. Sun, W., Fish, J., Ben, Dhia H.: A variant of the s-version of the finite element method for concurrent multiscale coupling. *Int. J. Multiscale Comput. Eng.* **16**(2), 197–207 (2018). <https://doi.org/10.1615/IntJMultCompEng.2018026400>
39. Vershinin, A., Levin, V., Zingerman, K., Sboychakov, A., Yakovlev, M.: Software for estimation of second order effective material properties of porous samples with geometrical and physical nonlinearity accounted for. *Adv. Eng. Softw.* **86**, 80–84 (2015). <https://doi.org/10.1016/j.advengsoft.2015.04.007>
40. Vdovichenko, I., Yakovlev, M., Vershinin, A., Levin, V.: Calculation of the effective thermal properties of the composites based on the finite element solutions of the boundary value problems. *IOP Conf. Ser. Mater. Sci. Eng.* **158**(1), 0212094 (2016). <https://doi.org/10.1088/1757-899X/158/1/012094>

-
41. Wu, Y., Lin, C., Yan, W., Liu, Q., Zhao, P., Ren, L.: Pore-scale simulations of electrical and elastic properties of shale samples based on multicomponent and multiscale digital rocks. *Mar. Pet. Geol.* **117**, 104369 (2020). <https://doi.org/10.1016/j.marpetgeo.2020.104369>
 42. Yvonnet, J., He, Q.C.: The reduced model multiscale method (R3M) for the non-linear homogenization of hyperelastic media at finite strains. *J. Comput. Phys.* **223**, 341–368 (2007). <https://doi.org/10.1016/j.jcp.2006.09.019>

Publisher's Note Springer Nature remains neutral with regard to jurisdictional claims in published maps and institutional affiliations.